# Closer look at the unitary evolution in radical-pair mechanism (report / journal)

Andrei Tretiakov

August 26, 2022

**Abstract**

The purpose of this manuscript is to summarize the results of my attempts to understand the quantum dynamics of the radical-pair mechanism allegedly responsible for magneto-reception in some bird species. The main goal is to develop an experimental protocol to extract meaningful information about the radical-pair mechanism in the total internal reflection fluorescence microscopy experiment. The document is written in a relatively free report/thesis/journal style to provide details that otherwise might have been omitted in a peer-review journal with a strict word limit and without an unnecessarily long introduction with a hundred references. The present document is based on my understanding of the field as of Summer 2022.

## 1 Introduction

After my first encounter with quantum biology about two years ago, I was astonished to learn that it is still not known how migratory bird species navigate. Especially considering the scale of scientific effort that lead to recent breakthroughs in our understanding of gravity, particle physics, and manipulating quantum matter, the fact that we do not understand such mundane, trivial, and yet ubiquitous subject as birds make me justifiably angry. While it is always compelling, intriguing, and crucial to go after the secrets of the universe, maybe it will make more sense to start with the world just in front of us?

Providentially, the topic might be related to the currently (over?)hyped field of quantum science, which can justify spending some research effort baked by the taxpayers' money on the problem. As it turns out, applying a magnetic field to some birds during their migratory period affects their flight direction [WW96], suggesting that they at least partially use the geomagnetic field for navigation. The fact that birds navigate with the help of the geomagnetic field is not that surprising, since even nowadays compass is the main component of human navigation. However, the details of the bird compass operation are still an open question that can potentially be solved with the help of quantum mechanics.

In-vivo experiments suggest that the avian compass is sensitive to magnetic field inclination [WW72] but not the polarity, meaning that the birds can distinguish between a geomagnetic pole and the equator but can not distinguish the two poles from each other. In addition, the compass efficiency depends on the frequency of light seen by the bird [WW95, WW99]. Finally, it was demonstrated that applying a weak magnetic field oscillating at an angle with respect to the geomagnetic field can disrupt the bird compass operation [RTP+04] provided that the oscillation frequency matches the frequency of an electron's spin Larmor precession in the geomagnetic field [RWH+09]. Based on this evidence, one of the most promising mechanisms explaining the bird compass operation is the radical-pair mechanism (RPM) [RAS00] described below.

## 2 Radical-pair mechanism

A radical is a molecule, atom, or ion with at least one unpaired electron. There are several situations where the creation of radical pairs takes place, but in the context of magneto-sensing, a radical pair (RP) is essentially a pair of spatially-separated entangled electrons' spins created inside a protein via a photo-induced electron transfer between parts of the protein. The most popular family of proteins in bio magneto-reception studies are cryptochromes. Inside these proteins, after absorbing a photon,

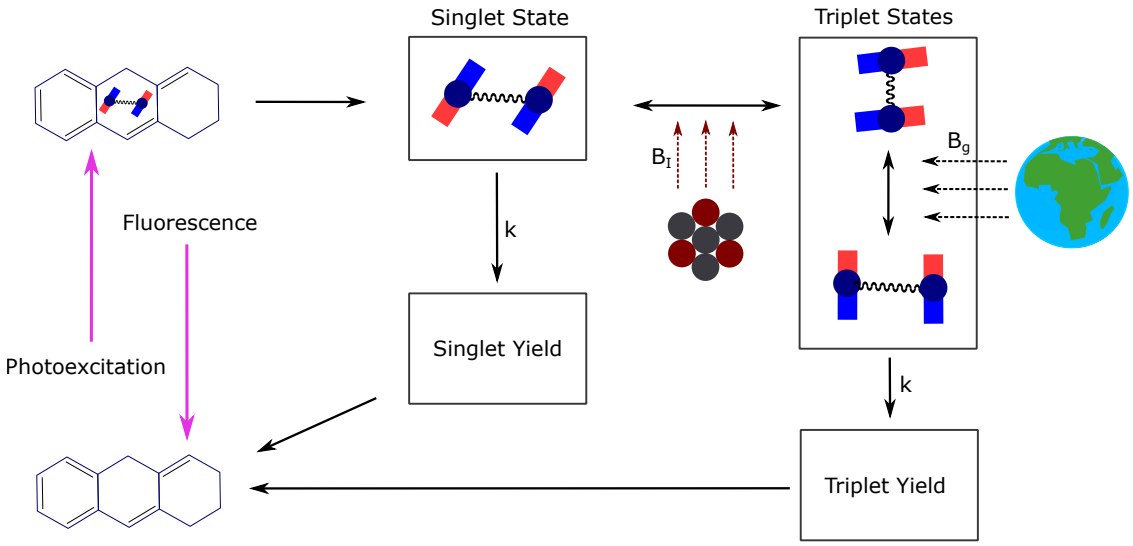


Figure 1: Schematics of the radical-pair mechanism as a basis for magnetoreception. The angle between the geomagnetic field and the internal nuclear reference affects the amount of time the radical pair spends between the triplet and singlet states and, as a result, the ratio of singlet to triplet yields which serves as a signal for the bird.

an electron is transferred from a Tryptophane (TrpH) to a photosensitive flavin adenine dinucleotide co-factor (FAD) [SDS14] separated from TrpH by about 2 nm [HM16]. The transfer process is spin preserving, so the transferred electron stays spin-entangled with the remaining unpaired electron in TrpH, and a radical pair is created. Since the two electrons are in a singlet state (total spin is zero) before the excitation, the radical pair is also created in a singlet state. Due to interaction with the internal magnetic field created by nuclear spins[1] and an external magnetic field, the RP can transfer between a singlet and a triplet (total spin is one) states, which is usually referred to as "singlet-triplet interconversion." The radical pair has a finite lifetime as the protein eventually undergoes chemical recombination, whose result depends on the quantum state of the radical pair, i.e., whether it was in a singlet (the two spins are always anti-aligned) or a triplet (spins are aligned) state. We use a simplified RPM model [GRM+11, PKSG17] schematically depicted in Figure 1, where are assume that singlet and triplet states collapse to produce different yields, but their collapse rates are the same.

### 2.1 My recommended references

For a brief introduction to the radical pairs I recommend Refs. [RAS00] and [HM16]. A thorough description of a radical pair creation process in cryptochrome can be found in Refs. [SDSS12] and [SDS14]. A detailed RPM model can be found in Ref. [SS12].

## 3 Hamiltonian

### 3.1 Intro

This section is a result of my attempt to understand quantum evolution in the RPM and how the interaction with an external magnetic field in the imbalance in singlet and triplet yields. I discovered that under some assumptions, the conventional radical-pair Hamiltonian written explicitly in terms of the singlet and triplet states provides some useful insights into the RPM. For me, an atomic physicist, working with the RPM Hamiltonian was a source of substantial joy, as adding just a single spin to a very familiar single-electron atom Hamiltonian resulted in a wide variety of new quantum effects.

[1] Since it is an established jargon in the field of quantum science, we will refer to both the angular and magnetic-dipole moments of electrons and nuclei as spins.

In general, the dynamics of the RP spins $\hat{\mathbf{S}}_1$ and $\hat{\mathbf{S}}_2$ in a uniform magnetic field $\mathbf{B}$ is governed by a rather complicated Hamiltonian given by [SSW+76]

$$\hat{H} = \mu_{\mathrm{B}}\mathbf{B}\cdot\left(g_1\hat{\mathbf{S}}_1 + g_2\hat{\mathbf{S}}_2\right) + \sum_k \hat{\mathbf{S}}_1\cdot\hat{A}_{1k}\cdot\hat{\mathbf{I}}_k + \sum_l \hat{\mathbf{S}}_2\cdot\hat{A}_{2l}\cdot\hat{\mathbf{I}}_l + J\left(\frac{1}{2} + 2\hat{\mathbf{S}}_1\cdot\hat{\mathbf{S}}_2\right),$$

where $\mu_{\mathrm{B}}$ is Bohr's magneton, and $g_1$ and $g_2$ are the electrons' gyromagnetic factors. Here, the first term corresponds to the Zeeman energy, and the second and the third terms describe the hyperfine interactions between the electrons and the magnetic field created by their surrounding nuclear spins $\hat{\mathbf{I}}_k$ and $\hat{\mathbf{I}}_l$, expressed via the hyperfine tensors $\hat{A}_{1k}$ and $\hat{A}_{2k}$. The last term corresponds to the exchange interaction between the two electron spins quantified by constant $J$.

In the context of biomagnetoreception, it is sufficient to consider a simplified model with the exchange interaction is neglected, and only a single electron interacts with the nuclear magnetic fields [RWH+09]. We will consider a model theoretically studied in Refs. [GRM+11, PKSG17] with the Hamiltonian given by

$$\hat{H} = 2\mu_{\mathrm{B}}\left(\hat{\mathbf{S}}_1 + \hat{\mathbf{S}}_2\right)\cdot\mathbf{B} + \hat{\mathbf{S}}_1\cdot\hat{A}\cdot\hat{\mathbf{I}}.$$

It is convenient to choose the coordinate system so that the hyperfine tensor is diagonal, in which case the hyperfine interaction is given by

$$\hat{\mathbf{S}}_1\cdot\hat{A}\cdot\hat{\mathbf{I}} = A_x\hat{S}_{1x}\hat{I}_x + A_y\hat{S}_{1y}\hat{I}_y + A_z\hat{S}_{1z}\hat{I}_z,$$

where $A_x, A_y, A_z$ are the eigenvalues of $\hat{A}$.

In the literature, the RPM dynamics is typically described using the basis consisting of a singlet state $|S\rangle$ and three triplet states $|T_0\rangle$, $|T_\uparrow\rangle$ and $|T_\downarrow\rangle$ corresponding to different projections onto the $z$-axis, and given by

$$|S\rangle = \frac{|\uparrow\downarrow\rangle - |\downarrow\uparrow\rangle}{\sqrt{2}},\ |T_0\rangle = \frac{|\uparrow\downarrow\rangle + |\downarrow\uparrow\rangle}{\sqrt{2}},\ |T_\uparrow\rangle = |\uparrow\uparrow\rangle,\ |T_\downarrow\rangle = |\downarrow\downarrow\rangle.$$

The full quantum state of the RP system in this model is described by a tensor product of the RP and the nuclear spin states. The quantum evolution is obtained by solving the Lindblad master equation

$$\frac{d}{dt}\hat{\rho} = -\frac{i}{\hbar}\left[\hat{H},\hat{\rho}\right] + \frac{1}{2}\sum_n\left(2\hat{L}_n\hat{\rho}\hat{L}_n^\dagger - \hat{\rho}\hat{L}_n^\dagger\hat{L}_n - \hat{L}_n^\dagger\hat{L}_n\hat{\rho}\right), \tag{1}$$

where $\hat{\rho}$ is the density matrix and $\hat{L}_n$ is the collapse operator due to a relaxation process $n$. Assuming all RP states recombine at the same rate $k$, the collapse operators are given by

$$\hat{L}_1 = \sqrt{k}\,|SY\rangle\langle S|,\ \hat{L}_2 = \sqrt{k}\,|TY\rangle\langle T_0|,\ \hat{L}_3 = \sqrt{k}\,|TY\rangle\langle T_\uparrow|,\ \hat{L}_4 = \sqrt{k}\,|TY\rangle\langle T_\downarrow|,$$

where $|SY\rangle$ and $|TY\rangle$ are the states corresponding to the singlet and triplet yields, respectively. The radical pair is presumed to originate in the singlet state, while the nuclear spin is typically presumed to be in a fully unpolarized state $0.5\,|\uparrow_I\rangle\langle\uparrow_I| + 0.5\,|\downarrow_I\rangle\langle\downarrow_I|$.

## 3.2 Better Hamiltonian

For the radical-pair mechanism to serve as a compass, a spatial reference should be related to the bird's orientation in space. In our model, such reference is provided by the hyperfine tensor, which is determined by the fixed geometry and orientation of the protein inside the bird's eye. In order to provide a reference axis, the hyperfine interaction has to be anisotropic. A typical hyperfine tensor considered in the literature has a cigar shape, i.e., $A_z = 2A_x = 2A_y$. In this case, the anisotropic part $A_z$ turns RPM into a compass by providing a reference axis along $z$, while the isotropic parts $A_x$ and $A_y$ actually reduce the compass efficiency. To better understand the compass mechanics, we will focus only on $A_z$ and assume that $A_x = A_y = 0$. Moreover, we will rewrite the hyperfine term as interaction

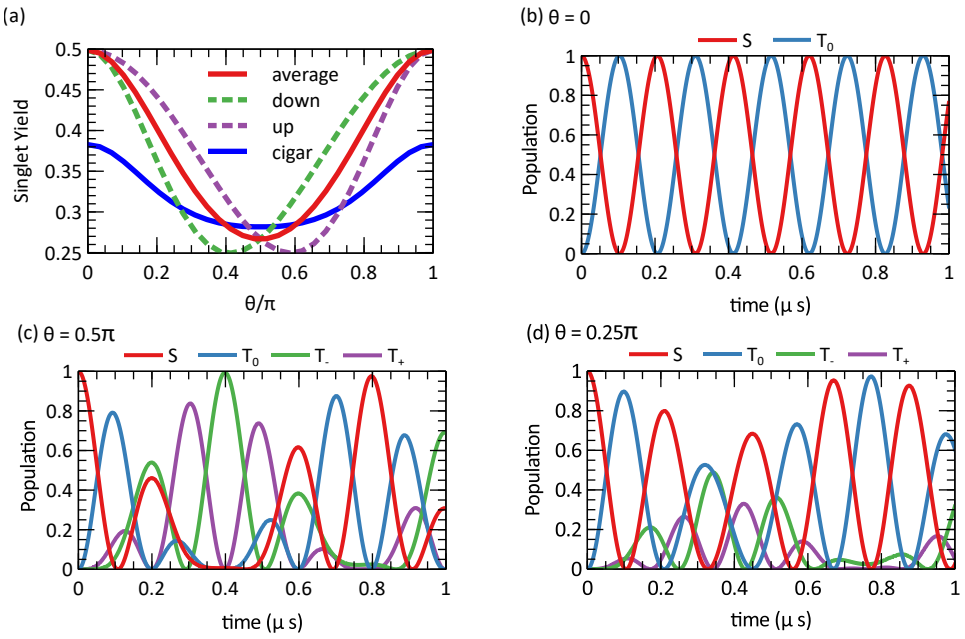


Figure 2: (a) Simulated singlet yield as a function of the angle between the nuclear axis and geomagnetic field. Dashed lines show the result for two orientations of the nuclear magnetic field with respect to $z$-axis. Red curve shows the average value of yield between the two nuclear field orientation. Blue curve shows the result in case of a cigar-shaped hyperfine interaction. (b, c, d) Simulated population of the singlet and triplet states in the absence of recombination for $\theta = 0$, $\theta = 0.5\pi$, and $\theta = 0.25\pi$. All simulations are done assuming $B = 47$ $\mu$T, $B_I = 3.68B$, $k = 10^4$ s$^{-1}$.

with an effective uniform nuclear field $B_I$: $A_z\hat{I}_z \to 2\mu_\mathrm{B}B_I$, which determines the compass reference axis. The Hamiltonian in this case becomes[2]

$$\hat{H}/2\mu_\mathrm{B} = \left(\hat{S}_{1x} + \hat{S}_{2x}\right) B_x + \left(\hat{S}_{1z} + \hat{S}_{2z}\right) B_z + \hat{S}_{1z}B_I,$$

where, without loss of generality, we assumed that the external magnetic field vector is in the $xz$ plane.

As mentioned before, we consider the nuclear spin to be in an unpolarized state $\hat{\rho}_I = \frac{1}{2}\hat{\mathbb{1}}_I$. In terms of an ensemble, this is equivalent to having half of the nuclear spins oriented along the reference axis and the other half oriented in the opposite direction. In the nuclear field model, the total contribution from a non-polarized nuclear ensemble can be reproduced by solving the Lindblad equation for two opposite orientations of the nuclear field and finding the average value of the yields in these two cases. Figure 1(a) shows the singlet yield dependence on the angle $\theta$ between $z$-axis and the static field simulated with the nuclear field approach has the same shape as in the case when the hyperfine interaction is described in terms of an unpolarized nuclear spin with a cigar-shaped hyperfine tensor. We also note that if we simulate the case of $A_x = A_y = 0$ with an unpolarized nuclear spin, it gives exactly the same result as the average yield in the case of the nuclear field (not shown).

Because the RPM recombination dynamics are described in terms of the singlet and triplet states, it makes perfect sense to rewrite the Hamiltonian using these states as the basis. And this is what we get[3]:

$$\hat{H}/2\mu_\mathrm{B} = B_I\left(|T_0\rangle\langle S| + \mathrm{h.c.}\right) + \frac{B_x}{\sqrt{2}}\left(|T_0\rangle\langle T_\uparrow| + |T_0\rangle\langle T_\downarrow| + \mathrm{h.c.}\right) + \left[B_z + B_I\right]\left(|T_\uparrow\rangle\langle T_\uparrow| - |T_\downarrow\rangle\langle T_\downarrow|\right).$$

[2]If I'd become a mathematician, this equation might be written using another notation for the Hamiltonian, like $\hat{H}'$ or $\hat{\hat{H}}$. "But I didn't, so it doesn't." The same applies to all equations that follow.

[3]Dear reader, I am sorry, but I will not include the derivation since it will consume another page or two. Let's say that I left it as an exercise for you or that "this margin is too narrow."

So far, so good. However, as the second term suggests, this Hamiltonian can be further simplified if we replace $|T_{\uparrow\downarrow}\rangle$ with $|T_{\pm}\rangle = \frac{|\uparrow\uparrow\rangle \pm |\downarrow\downarrow\rangle}{\sqrt{2}}$, giving us

$$\hat{H}/2\mu_{\mathrm{B}} = B_I|T_0\rangle\langle S| + B_x\,|T_+\rangle\,\langle T_0| + (B_z + B_I)\,|T_-\rangle\,\langle T_+| + \mathrm{h.c.} \tag{2}$$

And this is where it gets interesting. First of all, let us take a moment to appreciate the simple and elegant form of Eq. 2. If I ever get a tattoo, it will probably be something like that. Second of all, considering that the RP starts in the singlet state, the new Hamiltonian suggests that the RP unitary evolution undergoes the following stages:

1. Transitions between $|S\rangle$ and $|T_0\rangle$ due to the hyperfine interaction.
2. Transitions between $|T_0\rangle$ and $|T_+\rangle$ due to the external field component orthogonal to the nuclear field.
3. Transitions between $|T_+\rangle$ and $|T_-\rangle$ due to the external field component parallel to the nuclear field combined with the hyperfine interaction.

Or schematically, it can be depicted as follows:

$$|S\rangle \overset{B_I}{\longleftrightarrow} |T_0\rangle \overset{B_x}{\longleftrightarrow} |T_+\rangle \overset{B_z+B_I}{\longleftrightarrow} |T_-\rangle$$

and this is the way it is illustrated in Figure 1.

Based on the above, the RPM can be explained as follows. If there is no external field orthogonal to the reference axis, the RP state oscillates between $|S\rangle$ and $|T_0\rangle$ [Figure 2(b)], spending on average the same time in both states, and thus the singlet and triplet yields are balanced. An orthogonal field allows the system to couple to $|T_+\rangle$ and $|T_-\rangle$, from which it can not directly come back to the singlet state. As a result, on average, the system spends more time in the triplet state [Figure 2(c, d)], and the singlet yield is reduced.

Because I have encountered some misconceptions and vague descriptions of the effect of the geomagnetic field on the singlet-triplet inter-conversion and the RPM in some literature, I would like to stress that no external magnetic field can turn singlet into a triplet or alter the relative orientation of the two spins in any way as long as it couples equally to both spins [4]. As is evident from Eq. 2, it is required that there is an internal field that couples only to one of the spins to cause transitions between the singlet and triplet states.

Finally, all states in Eq. 2 are entangled and have zero angular momentum projection onto the $z$-axis.

## 3.3 Some remarks on the approximation

### 3.3.1 Remark 1

When I presented the above results for our group meeting, Daniel Kattnig noticed that the nuclear field approximation becomes exact in the case when the hyperfine interactions are negligible, but the two spins have different gyro-magnetic ratios. In this case, the Hamiltonian is given by

$$\hat{H}/\mu_{\mathrm{B}} = \left(g_1\hat{\mathbf{S}}_1 + g_2\hat{\mathbf{S}}_2\right)\cdot\mathbf{B} = \hat{\mathbf{S}}_1\cdot\mathbf{B}'_I + g_2\left(\hat{\mathbf{S}}_1 + \hat{\mathbf{S}}_2\right)\cdot\mathbf{B},$$

where $\mathbf{B}'_I = (g_1 - g_2)\mathbf{B}$. Note that the nuclear field is parallel to the external field, so the singlet state couples only to $|T_0\rangle$, and the evolution is insensitive to the field orientation.

Another case where the approximation is exact is when the magnetic field is non-uniform, and the two electrons have different Zeeman energies. Provided that $g_1 = g_2 = 2$, the Hamiltonian is given by

$$\hat{H}/2\mu_{\mathrm{B}} = \left(\hat{\mathbf{S}}_1 + \hat{\mathbf{S}}_2\right)\cdot\mathbf{B} + \hat{\mathbf{S}}_1\cdot\delta\mathbf{B},$$

where $\delta\mathbf{B}$ is the difference between the magnetic field vectors experienced by the two electrons, and it effectively plays the role of the nuclear field. If the field has both uniform and non-uniform contributions, the non-uniform part provides a reference axis, while the uniform part leads to a compass signal depending on the angle with respect to the reference axis. I believe it will be interesting to arrange that in a lab by superimposing a fixed non-uniform field and a uniform field of controllable orientation.

[4] We consider other cases in Section 3.3.1

### 3.3.2 Remark 2

When preparing the manuscript, I found that a similar semi-classical approach was previously applied in Ref. [Sch82], where the hyperfine interaction was modeled as an interaction with a single classical vector representing the average nuclear spin. However, our approach is more rigorous and provides some insights on the singlet-triplet interconversion that are either not mentioned or even contradict that work.

Farhan Tanvir Chowdhury also mentioned that the semi-classical approach is described in Ref. [MH13]. However, despite what my PI might think, I do not have the time or energy to study this one in awful depth since it gets quite mathematical quite quickly. Yet, from what I can tell, they are using classical equations of motion to model the evolution in the RPM. As in the previous reference, I believe it does not capture the beautiful insights of our approach.

# 4 RF-induced disorientation

As was mentioned in the introduction, it has been experimentally observed that bird compass efficiency can drop when a radio-frequency (RF) magnetic is applied, even when its magnitude is several orders of magnitude lower than that of the geomagnetic field $\mathbf{B}_g$[5]. In this case, Eq. 2 is still valid, but $B_x$ and $B_z$ can become time-dependent. Inspired by Refs.[GRM+11, PKSG17], Figure 3(a) illustrates how the RP compass contrast is reduced when an RF always perpendicular to the static field is applied. Here we set the RF frequency $\omega_{rf}$ to be equal to the Larmor frequency of the geomagnetic field $\omega_g = 2\mu_B B_g/\hbar$. The experiments presented in Ref. [RWH+09] suggest the RF effect on the RP compass has a resonance behavior, which we will look at below.

## 4.1 RF resonance in the rotating-wave approximation

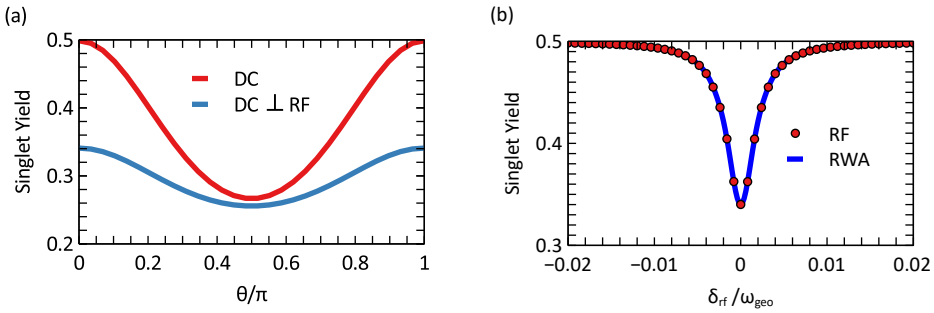


Figure 3: (a) Singlet yield as function of geomagnetic inclination in the DC case and RF cases. For the simulation, the RF field magnitude is $B_{rf} = 0.15$ $\mu$T, it is always perpendicular to the geomagnetic field, and $\omega_{rf} = \omega_g$ (b) RF resonance at $\theta = 0$. Other simulation parameters are the same as in Figure 2.

As can be seen in Fig. 3(a), the largest discrepancy between the static and RF cases occurs when the static field is parallel to the nuclear field. The time-dependent Hamiltonian in this situation is given by

$$\hat{H}_{rf}/2\mu_B = B_I|T_0\rangle\langle S| + B_{rf}\cos(\omega_{rf}t)\,|T_+\rangle\langle T_0| + (B_I + B_g)\,|T_-\rangle\langle T_+| + \text{h.c.} \tag{3}$$

For this particular case, it is convenient to consider the system evolution in a reference frame rotating around $z$-axis at a frequency $\omega_{rf}$ in the direction of the electron spin Larmor precession around the geomagnetic field. In terms of the Hamiltonian, it is equivalent to applying a fictitious magnetic field with magnitude $B_f$ satisfying $\omega_{rf} = \gamma B_f = 2\mu_B B_f/\hbar$ (for more rigorous treatment of the transformation to the rotating frame, see Ref. [CBDS94] and Ref [ZHS22]). The fictitious field is antialigned with

[5] Or the total external static field

the geomagnetic field, so the total field in the rotating frame is $B_z = \frac{\hbar}{2\mu_B}(\omega_g - \omega_{rf}) = -\frac{\hbar}{2\mu_B}\delta_{rf}$. The RF field in this frame has a static component $B_{rf}/2$ along $x$-axis and a component rotating around $z$-axis at twice the RF frequency in the direction opposite to the spin precession. Provided that the RF detuning $\delta_{rf}$ is sufficiently small, the effect of the rotating component on the spin dynamics averages out, and it can be excluded from the Hamiltonian, which is known as the rotating-wave approximation. Because the nuclear field is parallel to the rotation axis, the hyperfine term in the rotating frame is the same as in the laboratory frame. This leads to the rotating-wave Hamiltonian given by

$$\hat{H}_{rwa}/2\mu_B = B_I|T_0\rangle\langle S| + \frac{B_{rf}}{2}|T_+\rangle\langle T_0| + \left(B_I - \frac{\hbar}{2\mu_B}\delta_{rf}\right)|T_-\rangle\langle T_+| + \text{h.c.} \tag{4}$$

Figure 3(b) demonstrates that for $\theta = 0$, the singlet yield has resonant behavior and is greatly reduced when $\omega_{rf} = \omega_g$. The resonance shape calculated based on the rotating-wave approximation is in perfect agreement with the numerical simulations of the time-dependent case.

Some literature says that the RF field drives transitions between the singlet and triplet states leading to the disorientation.

# 5 Comparison of several numerical simulation approaches

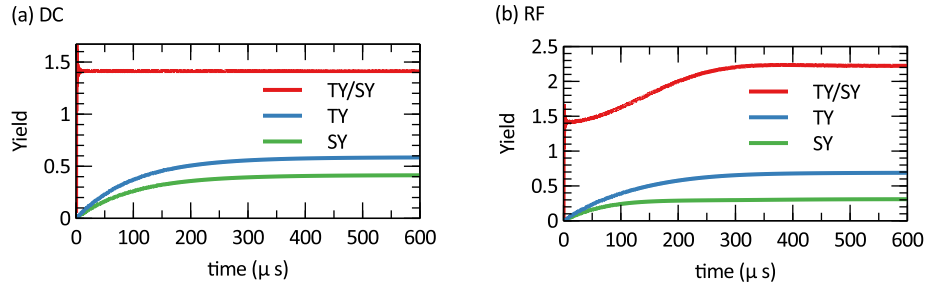


Figure 4: Singlet yield (SY), triplet yield (TY) and their ratios as a function of evolution time simulated for $\theta = \pi/4$. (a) Static case. (b) RF field is applied perpendicular to the geomagnetic field. The simulation parameters are the same as in Figure 2.

In the last section, I want to discuss several approaches to finding the singlet yield via numerical simulation that I was experimenting with in search of the most optimal method in terms of computational speed. Here, I have noticed some curious patterns that might have a physical origin, so I decided to include them in the manuscript.

The most straightforward and reliable approach is to solve the Lindblad equation with the evolution time sufficient for the recombination yields to reach their steady states, as is shown in Figure 4. The downside of this approach is that a larger evolution time corresponds to a larger computation time. One alternative is to use our insight on the connection between the singlet yield and the average singlet state population during the unitary evolution. This approach reproduces the data from Figure 2(a) with an evolution time of 10 $\mu$s instead of 600 $\mu$s for the steady-state approach. This allowed us to perform the computation based on 30 data points seven times faster. Finally, I have noticed that the ratio of singlet and triplet yields reaches its steady state much faster than the yields themselves, as is shown in Figure 4(a). Since the some of the steady-state yields adds up to one, both yields can be determined through their values at moment $t_S$ when the ratio reaches its steady-state as follows:

$$SY_S = \frac{SY(t_S)}{SY(t_S) + TY(t_S)}, \quad TY_S = \frac{TY(t_S)}{SY(t_S) + TY(t_S)}.$$

With this approach, I can reproduce Figure 2(a) using an evolution time of 10 $\mu$s, which computed five times faster than the original method.

Surprisingly, when I tried to reproduce the RF data from Figure 3(a) with the two new methods, they no longer provided accurate results when the evolution time is set to 10 $\mu$s. Figure 4(b) shows

that in the RF case, the triplet to singlet ratio levels off at the same rate as the individual rates, so the ratio-based method is no longer beneficial. I am not sure if it has any physical meaning, but if it was the case, it would be quite exciting to explore. The method bases on the average population does not seem to work in the RF case at all, regardless of how large I set the evolution time.

# 6 Conclusions

In this work, we applied the nuclear field approximation to the RPM Hamiltonian and expressed it explicitly in terms of the singlet and triplet states in a simple and compact form. This helped us to clearly identify the roles of the longitudinal and normal components of an external static magnetic field in the unitary evolution, especially their effect on the average time the system spends in a particular state, which in turn affects the corresponding recombination yield. Using the rotating wave approximation, we derived an analytical expression for the RF resonance in the case when the RF field has the most detrimental effect on the singlet yield. Finally, my simulations show that applying an RF field breaks down the connection between the average time spent in a particular state and its corresponding yield and the time it takes the singlet and triplet yield ratio to reach a steady state. If this effect is physical in origin, it might have significant consequences for understanding the RPM-based magnetoreception.

## 6.1 Possible experiments for the TIRF

- Experimentally reproduce Figure 3 (a). I think we can even train a deep neuronal network to identify the magnetic field based on the fluorescence image.
- Experimentally reproduce Figure 3 (b). The optimal static field direction will be determined from the previous step. Instead of varying RF frequency, it might be easier to vary the DC magnitude.
- By recording the fluorescence right after the excitation, try to reproduce Figure 4. As I understand, the fluorescence level is directly related only to the singlet yield, and I do not know if it is possible to measure the yield ratio somehow.

Note that the theoretical model that we used is oversimplified, so if the theoretical results can not be experimentally reproduced, that is possibly due to the limitations of the model. The next step from the point of view of theory is to study a more realistic model from Ref. [SDSS12].

# References


[CBDS94] J.M. Canfield, R.L. Belford, P.G. Debrunner, and K.J. Schulten. A perturbation theory treatment of oscillating magnetic fields in the radical pair mechanism. *Chemical Physics*, 182:1–18, 4 1994.

[GRM+11] Erik M. Gauger, Elisabeth Rieper, John J. L. Morton, Simon C. Benjamin, and Vlatko Vedral. Sustained quantum coherence and entanglement in the avian compass. *Physical Review Letters*, 106:040503, 1 2011.

[HM16] P. J. Hore and Henrik Mouritsen. The radical-pair mechanism of magnetoreception. *http://dx.doi.org/10.1146/annurev-biophys-032116-094545*, 45:299–344, 7 2016.

[MH13] D. E. Manolopoulos and P. J. Hore. An improved semiclassical theory of radical pair recombination reactions. *The Journal of Chemical Physics*, 139:124106, 9 2013.

[PKSG17] Vishvendra Singh Poonia, Kiran Kondabagil, Dipankar Saha, and Swaroop Ganguly. Functional window of the avian compass. *Physical Review E*, 95:052417, 5 2017.

[RAS00] Thorsten Ritz, Salih Adem, and Klaus Schulten. A model for photoreceptor-based magnetoreception in birds. *Biophysical Journal*, 78:707–718, 2 2000.

[RTP+04] Thorsten Ritz, Peter Thalau, John B. Phillips, Roswitha Wiltschko, and Wolfgang Wiltschko. Resonance effects indicate a radical-pair mechanism for avian magnetic compass. *Nature 2004 429:6988*, 429:177–180, 5 2004.

[RWH+09] Thorsten Ritz, Roswitha Wiltschko, P.J. Hore, Christopher T. Rodgers, Katrin Stapput, Peter Thalau, Christiane R. Timmel, and Wolfgang Wiltschko. Magnetic compass of birds is based on a molecule with optimal directional sensitivity. *Biophysical Journal*, 96:3451–3457, 4 2009.

[Sch82] Klaus Schulten. Magnetic field effects in chemistry and biology, 1982.

[SDS14] Ilia A. Solov'yov, Tatiana Domratcheva, and Klaus Schulten. Separation of photo-induced radical pair in cryptochrome to a functionally critical distance. *Scientific Reports 2014 4:1*, 4:1–8, 1 2014.

[SDSS12] Ilia A. Solov'Yov, Tatiana Domratcheva, Abdul Rehaman Moughal Shahi, and Klaus Schulten. Decrypting cryptochrome: Revealing the molecular identity of the photoactivation reaction. *Journal of the American Chemical Society*, 134:18046–18052, 10 2012.

[SS12] Ilia A. Solov'yov and Klaus Schulten. Reaction kinetics and mechanism of magnetic field effects in cryptochrome. *Journal of Physical Chemistry B*, 116:1089–1099, 1 2012.

[SSW+76] K. Schulten, H. Staerk, A. Weller, H.-J. Werner, and B. Nickel. Magnetic field dependence of the geminate recombination of radical ion pairs in polar solvents. *Zeitschrift für Physikalische Chemie*, 101:371–390, 9 1976.

[WW72] Wolfgang Wiltschko and Roswitha Wiltschko. Magnetic compass of european robins. *Science*, 176:62–64, 4 1972.

[WW95] W. Wiltschko and R. Wiltschko. Migratory orientation of european robins is affected by the wavelength of light as well as by a magnetic pulse. *Journal of Comparative Physiology A 1995 177:3*, 177:363–369, 9 1995.

[WW96] Wolfgang Wiltschko and Roswitha Wiltschko. Magnetic orientation in birds. *Journal of Experimental Biology*, 199:29–38, 1 1996.

[WW99] W. Wiltschko and R. Wiltschko. The effect of yellow and blue light on magnetic compass orientation in european robins, erithacus rubecula. *Journal of Comparative Physiology A 1999 184:3*, 184:295–299, 1999.

[ZHS22] Hadi Zadeh-Haghighi and Christoph Simon. Magnetic field effects in biology from the perspective of the radical pair mechanism. *Journal of The Royal Society Interface*, 19, 8 2022.